Supporting Information for:

One macrocyclic ligand, four oxidation states: A 16-atom ringed di-anionic tetra-NHC macrocycle and its Cr(II) through Cr(V) complexes

Markus R. Anneser, Xian B. Powers, KatieAnn M. Peck, Isabel M. Jensen, and David M. Jenkins*

Department of Chemistry, University of Tennessee, Knoxville, Tennessee 37996, United States

Table of contents:

1. NMR Data of Compounds **1** to **5**.

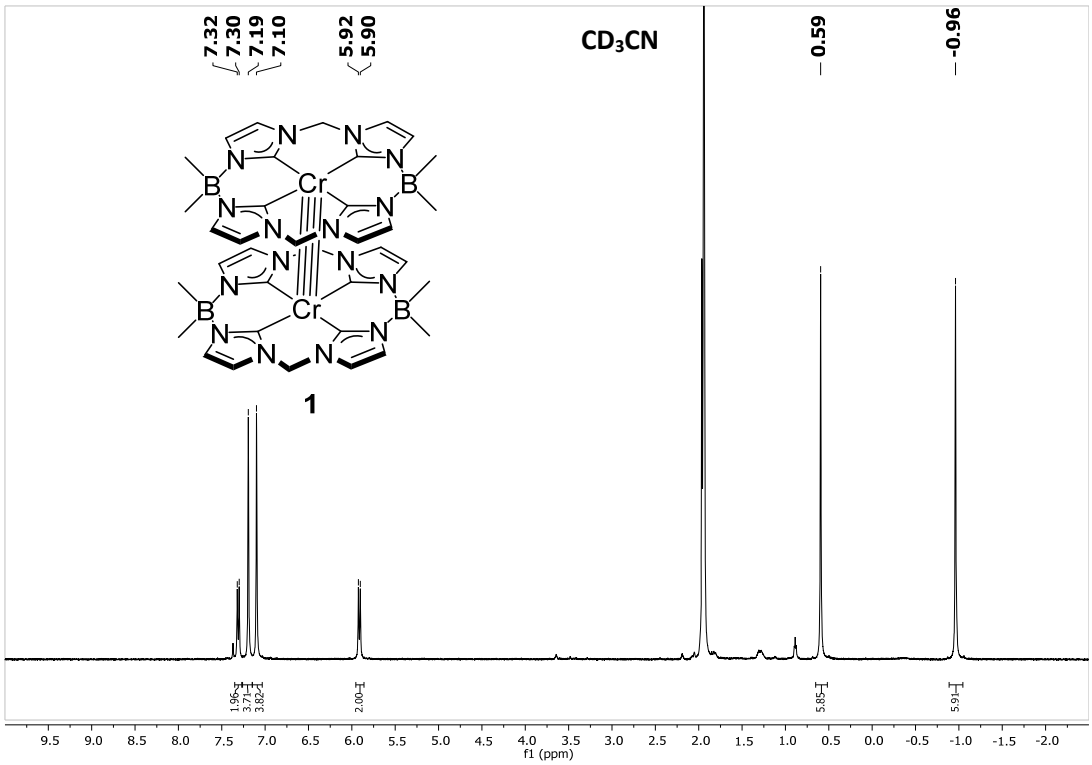

Figure S1: ^{1}H NMR of ((^{BMe_2,Me}TC^{H})Cr)$_2$ (**1**) in MeCN-d$_3$.

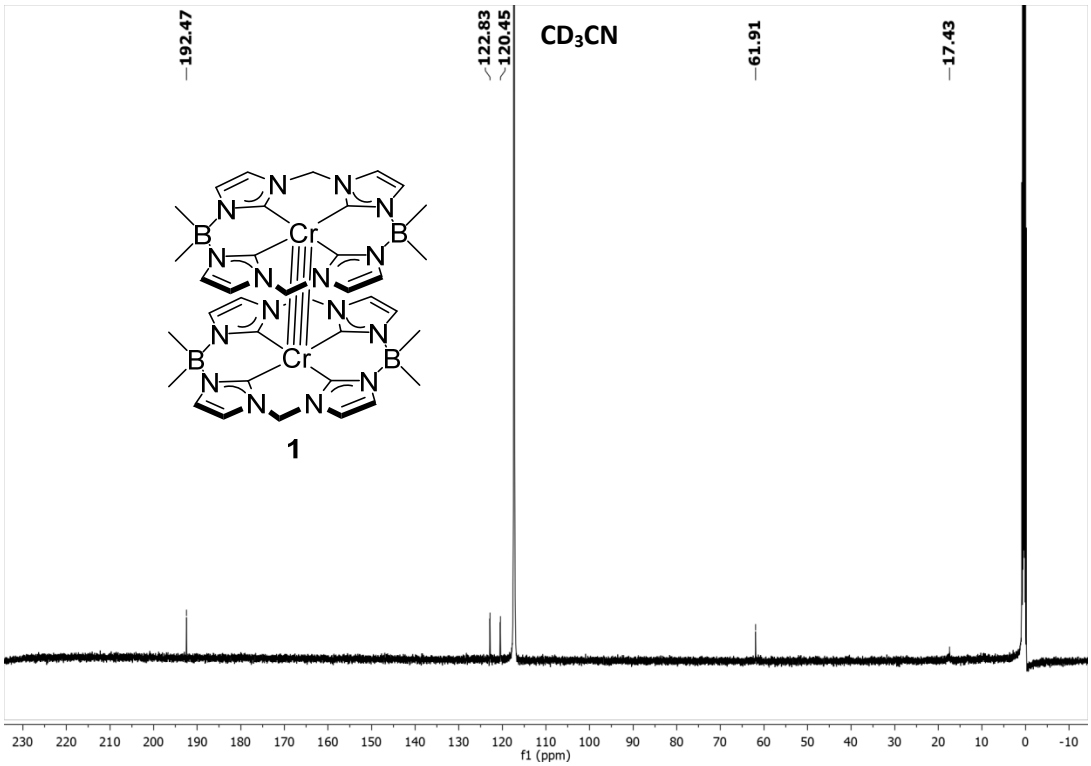

Figure S2: ^{13}C NMR of ((^{BMe_2,Me}TC^{H})Cr)$_2$ (**1**) in MeCN-d$_3$.
(peak at 9.5 ppm is very broad, see HSQC Fig.3)

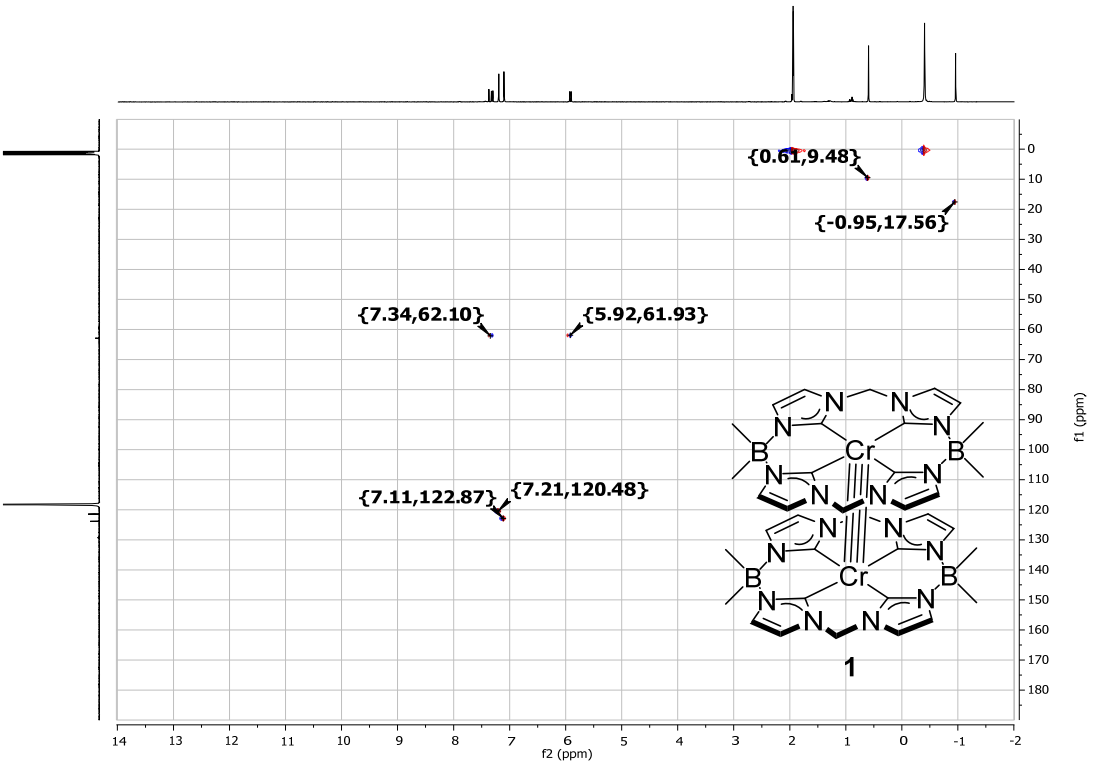

Figure S3: HSQC of (($^{BMe_2,Me}TC^{H}$)Cr)$_2$ (**1**) in MeCN-d$_3$.

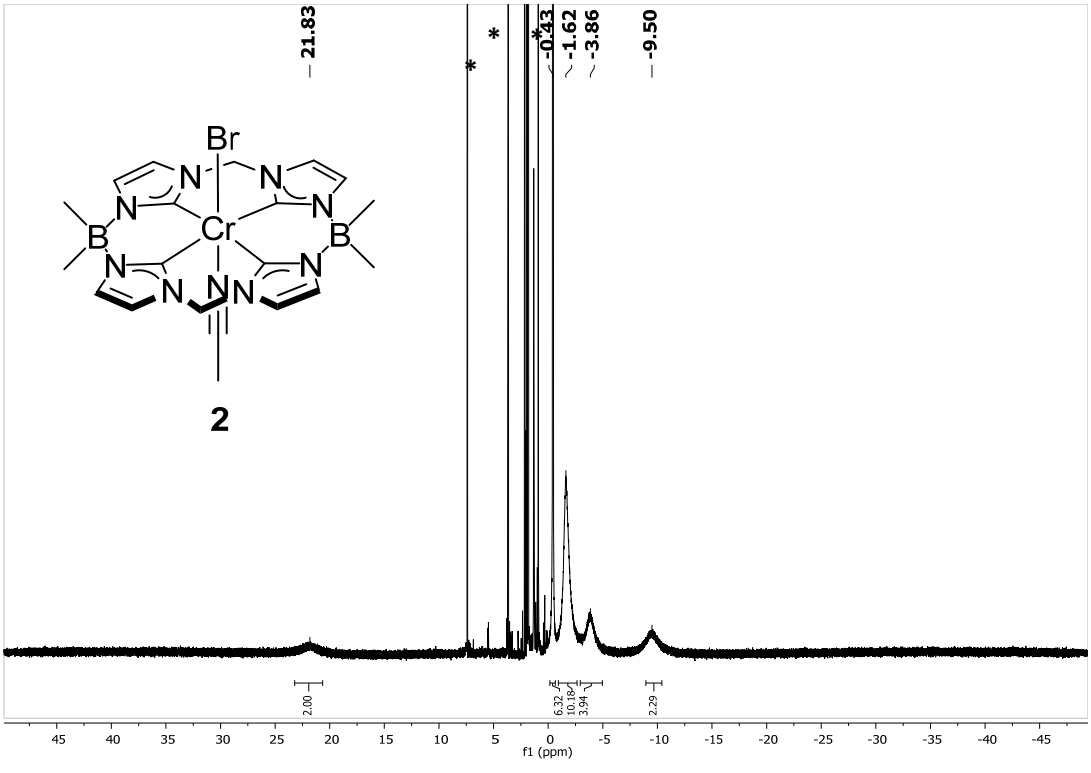

Figure S4: Paramagnetic ^{1}H NMR of ($^{BMe_2,Me}TC^{H}$)Cr(Br)(NCCH$_3$) (**2**) in MeCN-d$_3$, collected from 5 mg of crystalline solid (*).

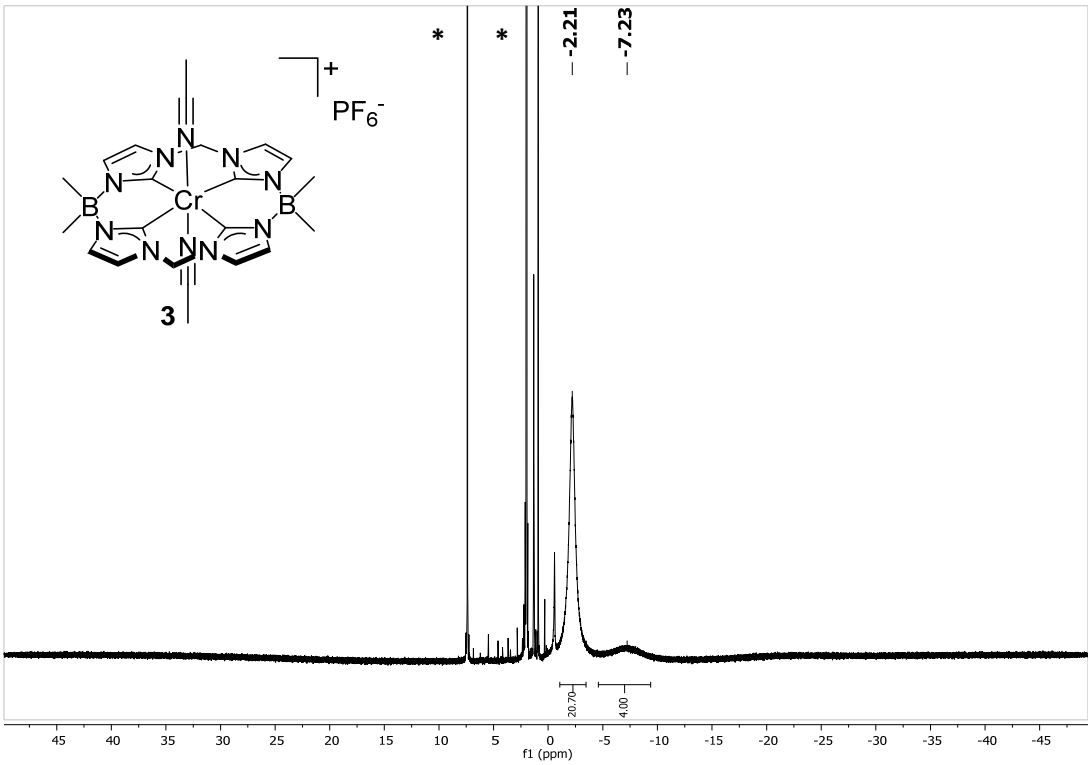

Figure S5: Paramagnetic ^{1}H NMR of [(^{BMe_2,Me}TC^{H})Cr(NCCH$_3$)$_2$](PF$_6$) (**3**) in MeCN-d$_3$, collected from 5 mg of crystalline solid grown from MeCN/benzene (*).

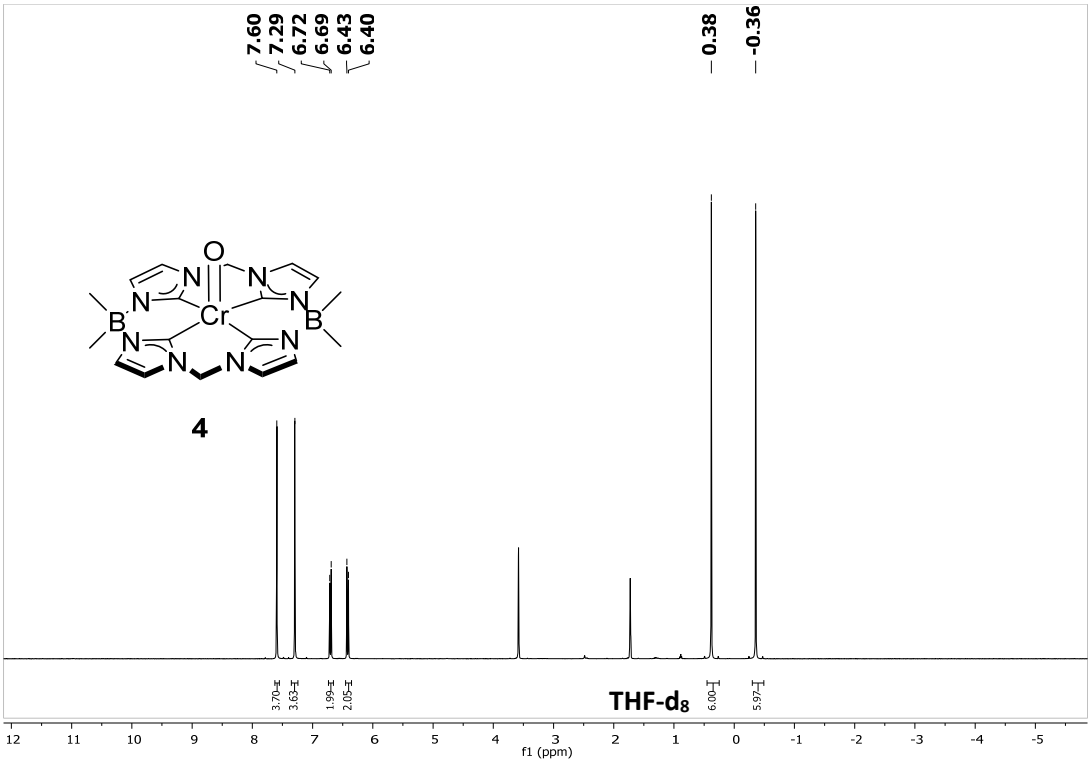

Figure S6: ^{1}H NMR of (^{BMe_2,Me}TC^{H})CrO (**4**) in THF-d$_8$.

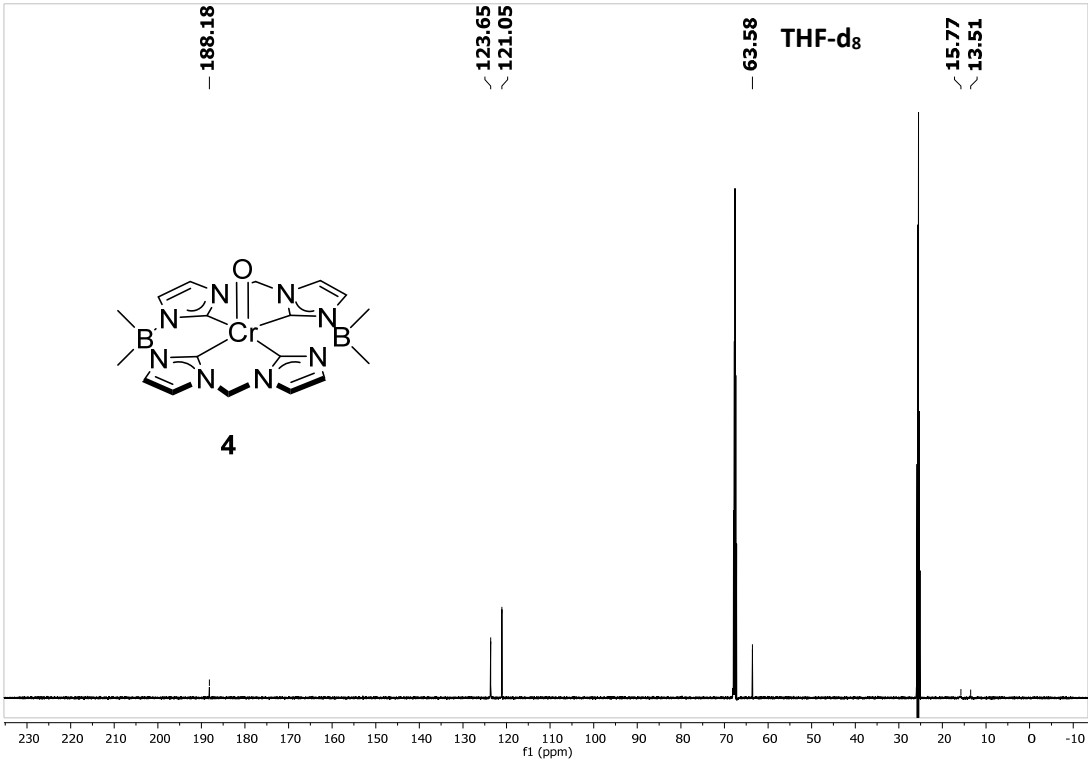

Figure S7: ^{13}C NMR of ($^{BMe_2,Me}TC^{H}$)CrO (**4**) in THF-d_8.

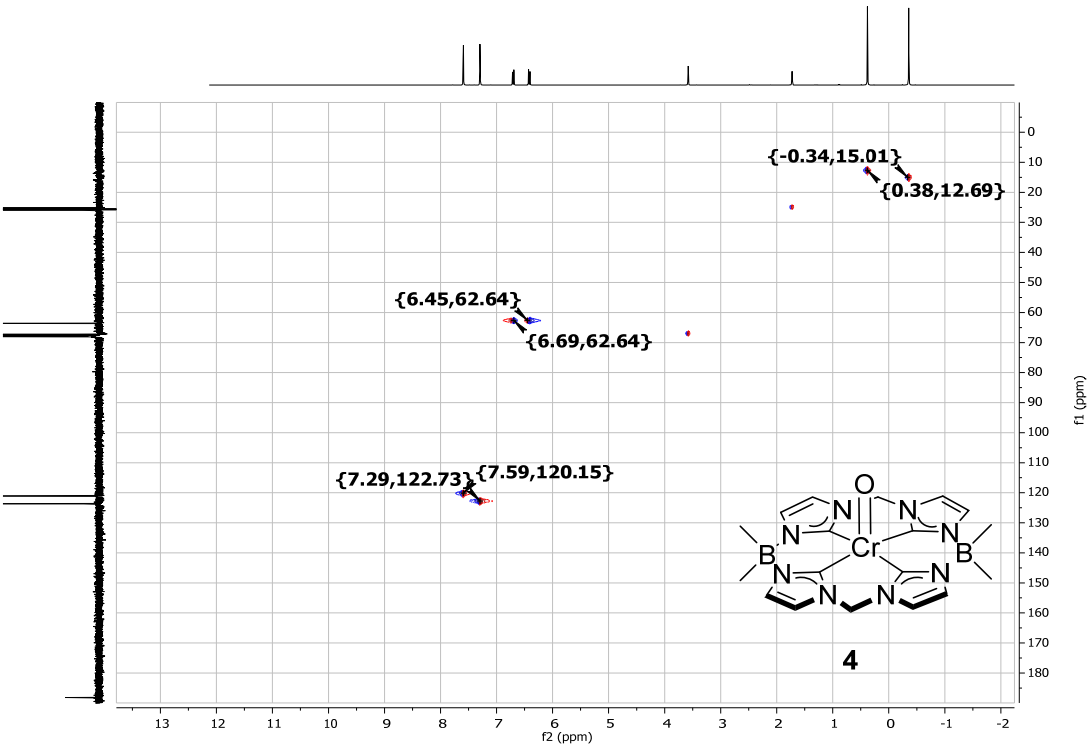

Figure S8: HSQC of ($^{BMe_2,Me}TC^{H}$)CrO (**4**) in THF-d_8.

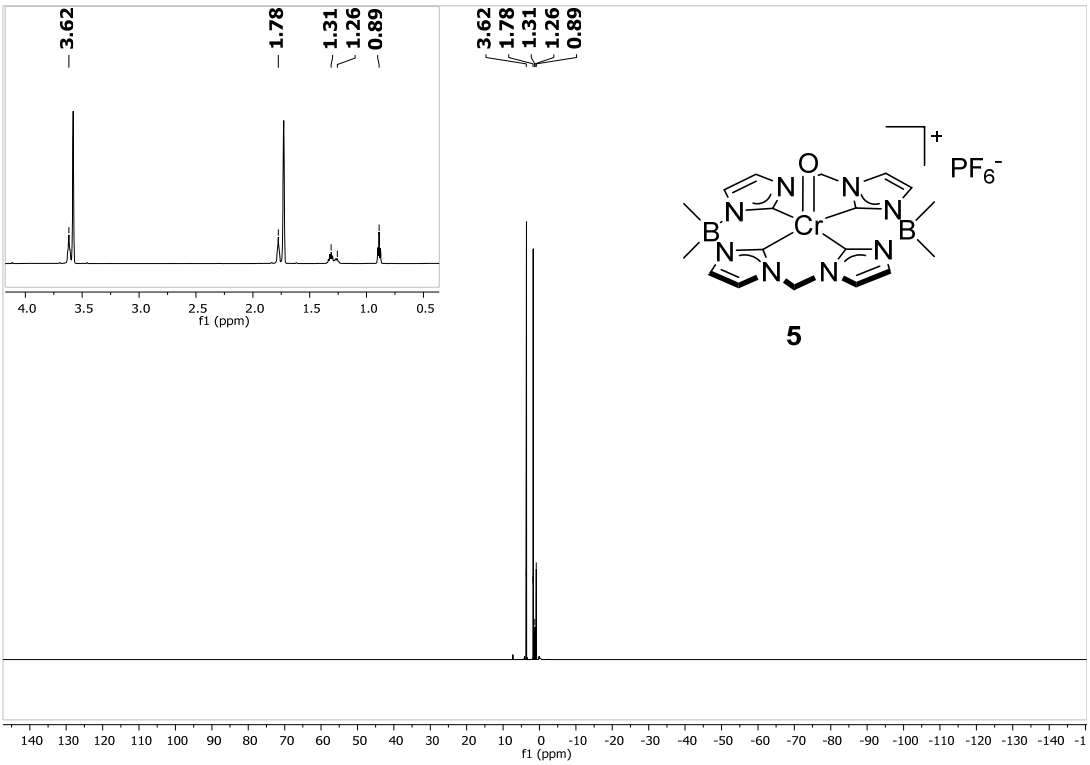

Figure S9: ^{1}H NMR of [(^{BMe2,Me}TC^{H})CrO](PF$_6$) (**5**) in THF-d$_8$, collected from 5 mg of crystalline solid grown from THF/pentane. No signals are observed.

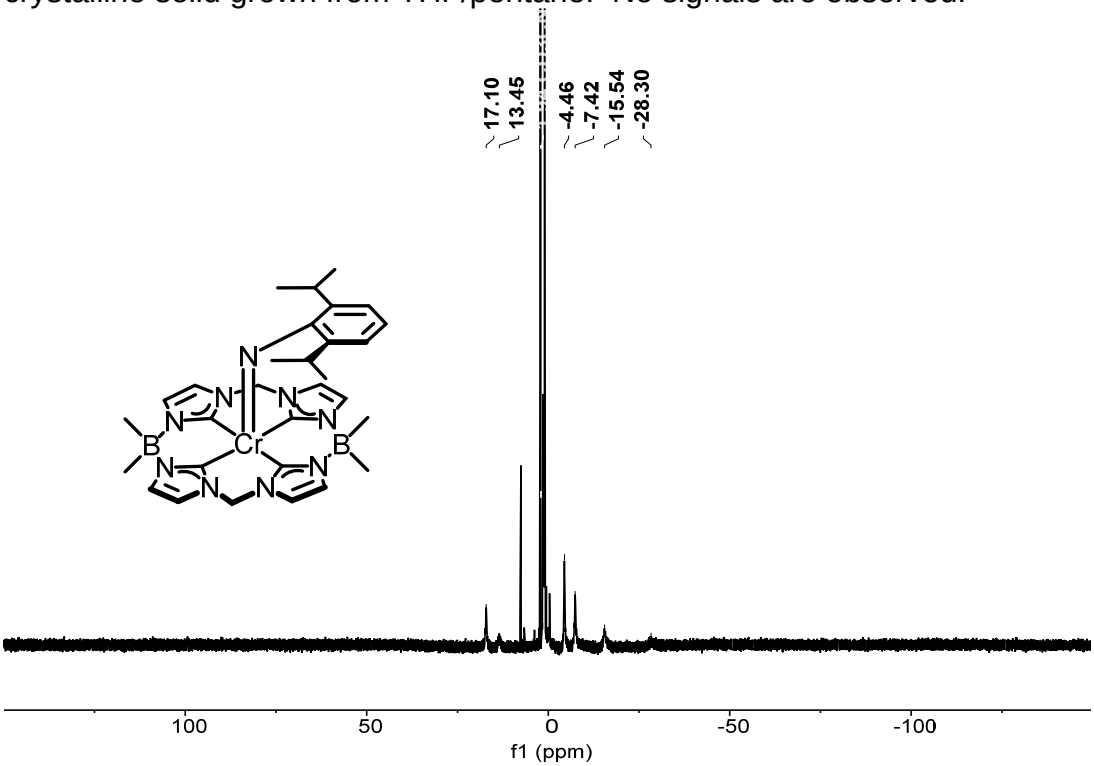

Figure S10: Paramagnetic ^{1}H NMR of (^{BMe2,Me}TC^{H})Cr(N(DiPP)) (**6**) in MeCN-d$_3$.

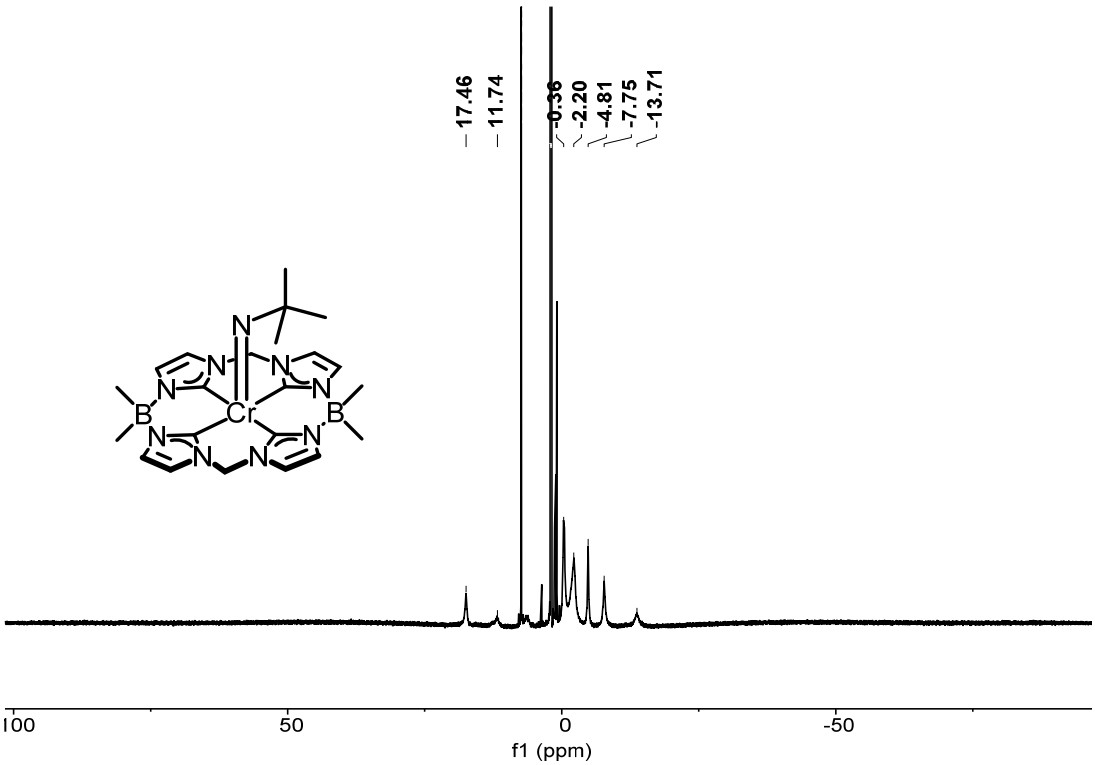

Figure S11: Paramagnetic ^{1}H NMR of ($^{BMe_2,Me}TC^{H}$)Cr(N^{t}Bu) (**7**) in MeCN-d_3.

2. Various NMR Data

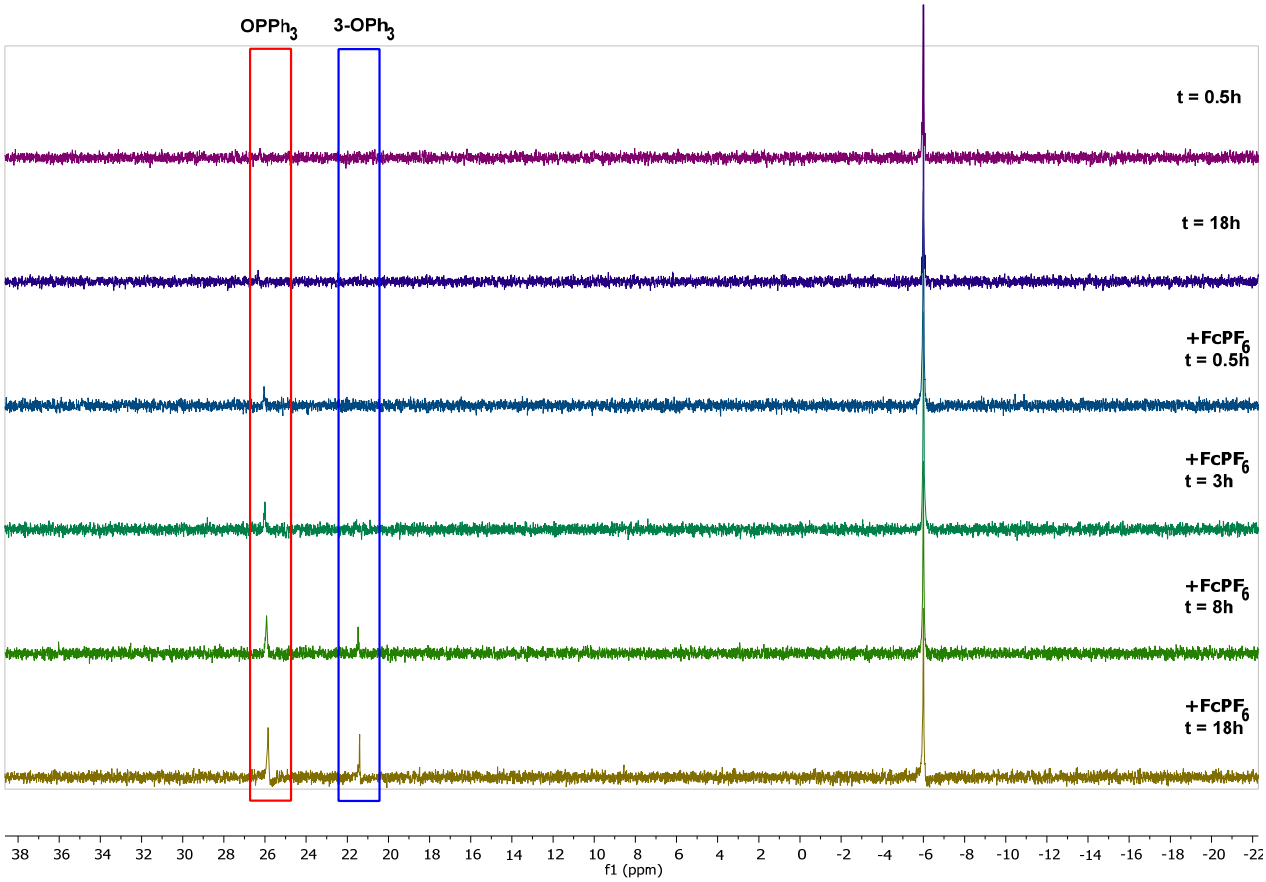

Figure S12: ^{31}P NMR of **4** with 2 equiv. PPh_3 in MeCN-d_3 before and after addition of 1 equiv. of $FcPF_6$, resulting in the oxidation of PPh_3 to $OPPh_3$ (26 ppm) via compound **5**. The peak evolving at 21.5 ppm is likely to be assigned to a $OPPh_3$ adduct as **3** accumulates.

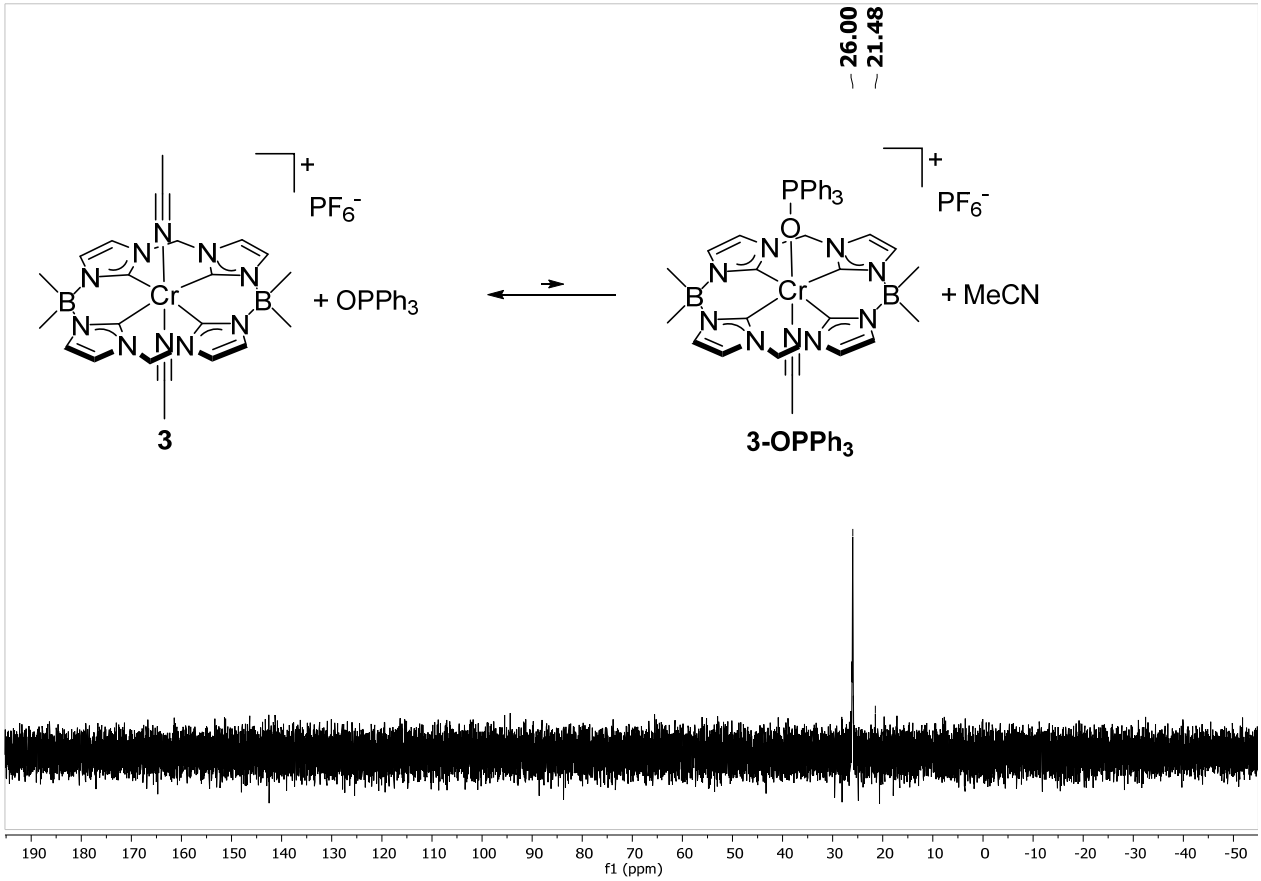

Figure S13: ^{31}P NMR of **3** with 1 equiv. $OPPh_3$ in MeCN-d_3. Small peak at 21.5 ppm indicates the formation of **3**-$OPPh_3$.

3. NMR data for Mo reactions

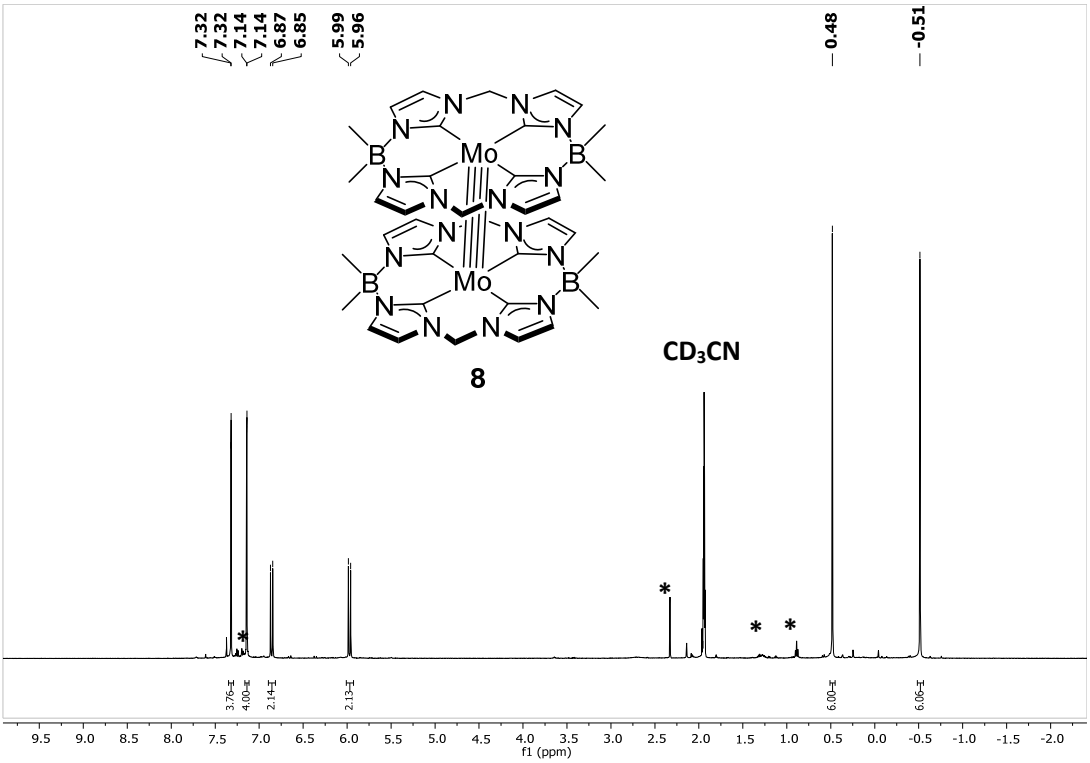

Figure S14: ^{1}H NMR of ((^{BMe_2,Me}TC^{H})Mo)$_2$ (**8**) in MeCN-d$_3$, collected from 2 mg of crystalline solid grown from toluene/pentane (*).

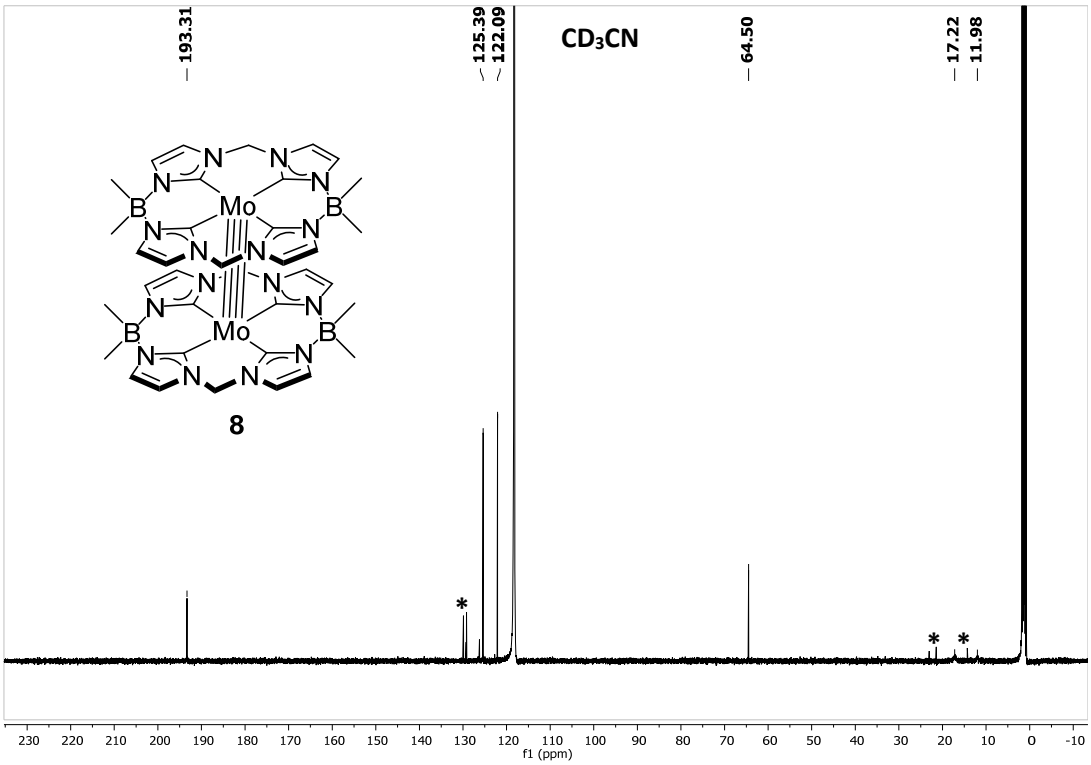

Figure S15: ^{13}C NMR of ((^{BMe_2,Me}TC^{H})Mo)$_2$ (**8**) in MeCN-d$_3$, collected from 2mg of crystalline solid grown from toluene/pentane (*).

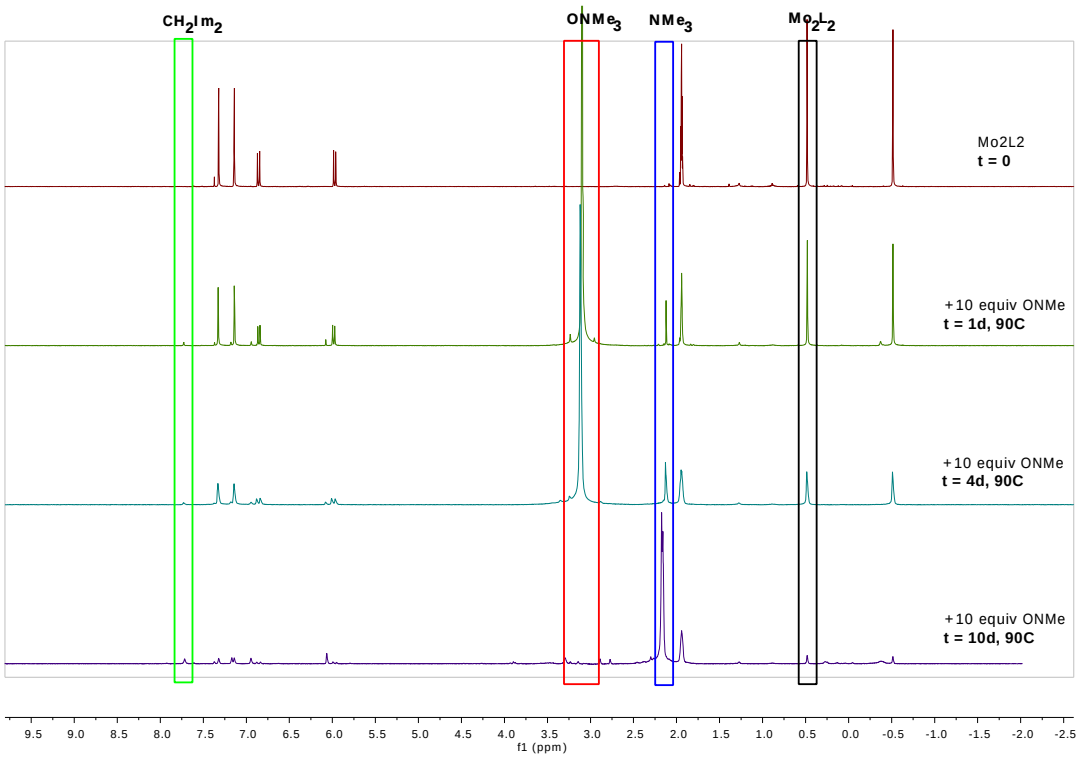

Figure S16: ^{1}H NMR of ($^{BMe_2,Me}TC^{H}$)Mo$_2$ (**8**) mixed with 10 equiv. of ONMe$_3$ in MeCN-d$_3$, heated to 90 °C in a sealed NMR tube for 1, 4 and 10 days.

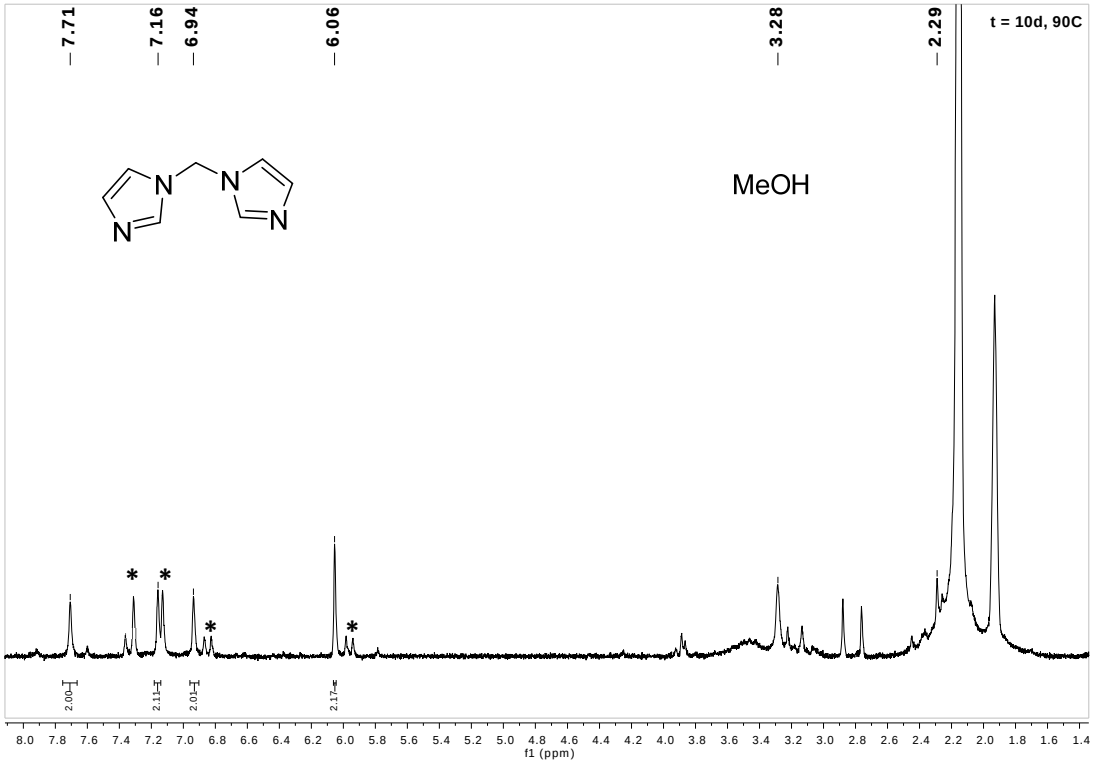

Figure S17: ^{1}H NMR of ($^{BMe_2,Me}TC^{H}$)Mo$_2$ (**8**) mixed with 10 eq. of ONMe$_3$ in MeCN-d$_3$, heated to 90 °C in a sealed NMR tube for 10 days. (*) are from residual **8**.

4. Cyclic Voltammetry Data

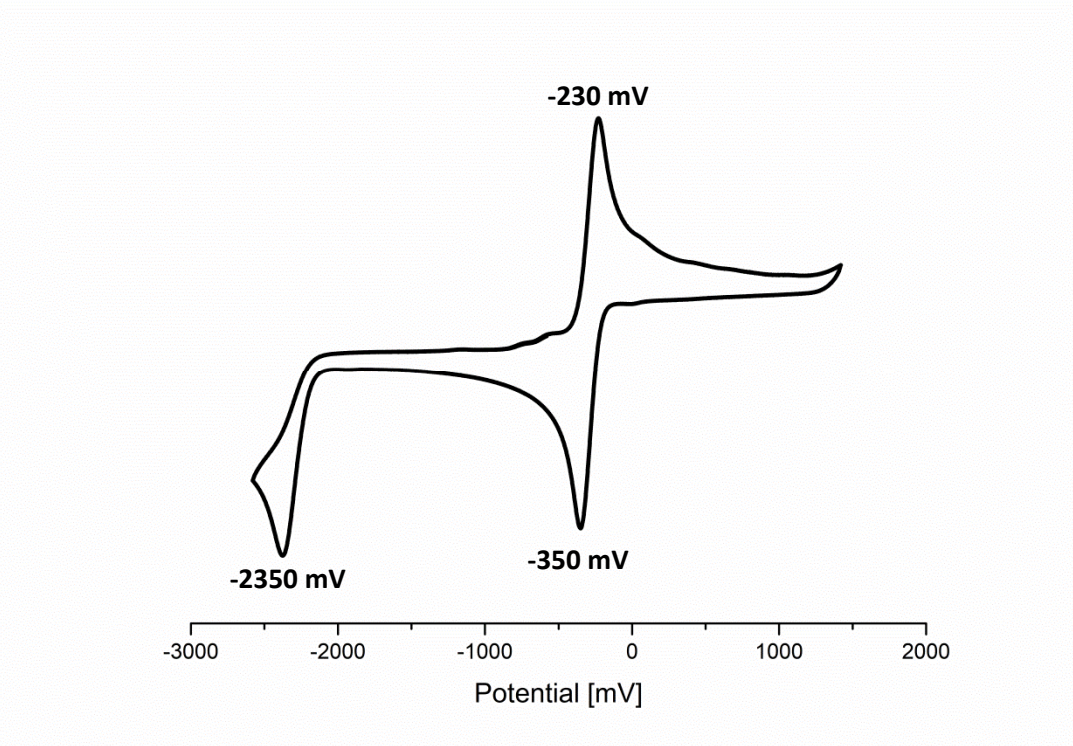

Figure S18: CV of **4** in MeCN (0.1 M $TBAPF_6$; 100 mV/s; Pt-Electrode).